Inorg. Chem. **2009**, *48*, 4067−4074

Synthesis, Structure, and Optical Properties of the Platinum(II) Complexes of Indaphyrin and Thiaindaphyrin

Kimberly S. F. Lau,[†,‡] Shengxian Zhao,[‡] Claudia Ryppa,[‡] Steffen Jockusch,[§] Nicholas J. Turro,[§] Matthias Zeller,[||] Martin Gouterman,[†] Gamal E. Khalil,[†] and Christian Brückner*[,‡]

Department of Chemistry, University of Washington, Box 351700, Seattle, Washington 98195-1700, Department of Chemistry, University of Connecticut, Unit 3060, Storrs, Connecticut 06269-3060, Department of Chemistry, Columbia University, New York, New York 10027, and Department of Chemistry, Youngstown State University, One University Plaza, Youngstown, Ohio 44555-3663

Received October 24, 2008

The novel free base *meso*-di(5′-methylthien-2′-yl)thiaindaphyrin, **10**, was prepared from the corresponding *meso*-tetra(thien-2-yl)porphyrin using a methodology analogous to that for the preparation of known *meso*-diphenylindaphyrin, **5**: β,β'-Dihydroxylation of the porphyrin is followed by oxidative diol cleavage. The resulting aldehyde moieties undergo an acid-catalyzed intramolecular Friedel−Crafts alkylation of the adjacent *meso*-thienyl groups with concomitant oxidation. Insertion of Pt(II) into either of the chromophores is facile, producing **5Pt** and **10Pt**. The crystal structure of **5Pt**, the first for any indaphyrin, shows that the conformation of the indaphyrinato ligand is strongly ruffled, while the N_4 donor set that coordinates the central Pt(II) maintains a near-perfect square-planar coordination geometry around the central metal ion (crystal data for $C_{44}H_{24}N_4O_2Pt$: triclinic space group $P\bar{1}$ with $a = 8.8735(4)$ Å, $b = 12.9285(6)$ Å, $c = 14.3297(6)$ Å, $\alpha = 88.785(1)°$, $\beta = 82.248(1)°$, $\gamma = 72.422(1)°$; $Z = 2$). The UV−vis and emission spectra, triplet yields, and lifetimes of the Pt(II) complexes **5Pt** and **10Pt** were determined. Both complexes luminesce (in EtOH at 77 K) in the NIR (**5Pt**: $\lambda_{max\text{-}emission} = 864$, 974 nm, lifetime 2 μs; **10Pt**: $\lambda_{max\text{-}emission} = 990$, 1112, 1276 nm) with modest to low quantum yields ($\Phi_p \sim 1\%$ and $\sim 6 \times 10^{-3}$ %, respectively).

Introduction

The triplet oxygen-mediated quenching of the triplet excited-state of many chromophores (Stern−Volmer quenching) allows a correlation between the degree of quenching and a particular oxygen partial pressure.[1] This gives rise to the development of optical oxygen sensors that find applications in medicine, engineering, and chemical and environmental analyses.[1−3]

One particularly well-studied class of compounds for oxygen sensing applications is that of the Pt(II) porphyrins, such as [*meso*-tetraphenylporphyrinato]Pt(II) (**1Pt**) and related compounds.[1,4−7] In Pt(II) and Pd(II) porphyrins, ligand-based emissions are observed ($\lambda_{max\text{-}emission}$ for **1Pt** = 650, 712

* To whom correspondence should be addressed. Phone: (860) 486-2743. Fax: (860) 486-2981. E-mail: c.bruckner@uconn.edu.
† University of Washington.
‡ University of Connecticut.
§ Columbia University.
|| Youngstown State University.

(1) Lakowicz, J. R. *Principles of Fluorescence Spectroscopy*, 3rd ed.; Springer: New York, 2006.
(2) Gouterman, M. *J. Chem. Educ.* **1997**, *74*, 697–702.
(3) (a) Leiner, M. J. P. *Anal. Chim. Acta* **1991**, *255*, 209–222. (b) Papkovsky, D. B.; O'Riordan, T.; Soini, A. *Biochem. Soc. Trans.* **2000**, *28*, 74–77.
(4) Xiang, H.-F.; Li, C.-N.; Yu, S. C.; Che, C.-M.; Lai, P. T.; Chui, P. C. *Proc. SPIE Int. Soc Opt. Eng.* **2004**, *5519*, 218–225.
(5) Vinogradov, S. A.; Lo, L.-W.; Wilson, D. F. *Eur. J. Chem.* **1999**, *5*, 1338–1347.
(6) Briñas, R. P.; Troxler, T.; Hochstrasser, R. M.; Vinogradov, S. A. *J. Am. Chem. Soc.* **2005**, *127*, 11851–11862.
(7) Huo, C.; Zhang, H.; Zhang, H.; Zhang, H.; Yang, B.; Zhang, P.; Wang, Y. *Inorg. Chem.* **2006**, *45*, 4735–4742.
(8) Gouterman, M.; Hall, R. J.; Khalil, G.-E.; Martin, P. C.; Shankland, E. G.; Cerny, R. L. *J. Am. Chem. Soc.* **1989**, *111*, 3702–3707.
(9) Zelelow, B.; Khalil, G. E.; Phelan, G.; Carlson, B.; Gouterman, M.; Callis, J. B.; Dalton, L. R. *Sens. Actuators, B* **2003**, *96*, 304–314.
(10) Gouterman, M.; Callis, J.; Dalton, L.; Khalil, G.; Mebarki, Y.; Cooper, K. R.; Grenier, M. *Meas. Sci. Technol.* **2004**, *15*, 1986–1994.
(11) Khalil, G. E.; Costin, C.; Crafton, J.; Jones, G.; Grenoble, S.; Gouterman, M.; Callis, J. B.; Dalton, L. R. *Sens. Actuators, B* **2004**, *97*, 13–21.

10.1021/ic802041z CCC: $40.75
Published on Web 04/02/2009

nm).[2] This allows a modulation of the excitation and emission wavelengths through alterations of the porphyrinic chromophore. Examples include the use of the Pd(II) and Pt(II) complexes of porpholactones, **2Pt**,[8−11] β-oxo-porphyrins,[12] or benzoporphyrins, such as complex **3Pt**.[13]

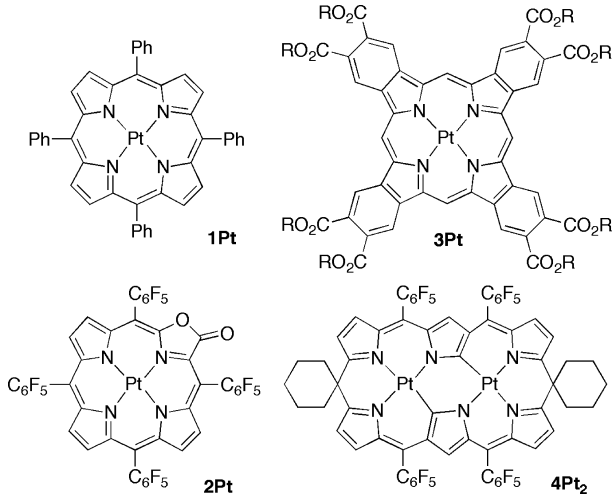

A red shift of the excitation or luminescence spectra into the red or NIR range ($\lambda_{\text{max-emission}} > 750$ nm) is desirable for a number of applications, particularly in the life sciences.[14] By utilizing red to near-infrared (NIR) wavelengths, an increase in the sensitivity of luminescence-based assays in biological systems measurements can be achieved because no natural chromophore emits in this region. The NIR is also the region of the "spectroscopic window" in tissue, and chromophores emitting in this range may allow the detection of events deep in the tissue. Last, longer wavelengths are scattered less in opaque media than shorter ones, increasing the resolution of the emission images obtained.

This emission red shift was the driving force behind the development of π-extended porphyrins such as **3Pt** ($\lambda_{\text{max-emission}} = 745$ nm)[15] or the bimetallic complex of an *N*-confused calyx[6]phyrin **4Pt$_2$** ($\lambda_{\text{max-emission}} = 1010$ nm).[16] An ideal sensor molecule should fulfill other key requirements such as high extinction coefficients and high emission quantum yields (i.e., possessing high brightness), and excellent photostability. Ancillary properties such as nonaggregation in a polymer matrix, good processability, and a large Stokes shift further improve their applicability.

We reported recently the synthesis of a novel class of porphyrin derivatives, the indaphyrins, **5**. This class of compounds, synthesized from *meso*-tetraphenylporphyrin, contains a β,β'-ring-cleaved pyrrole moiety. The former β-carbons have become ketone moieties that are fused to the *o*-position of the neighboring *meso*-phenyl rings, thus giving rise to the formation of indanone moieties.[17,18] It was computed that the short linkage forces the indanone groups into near coplanarity with the mean plane of the greatly ruffled porphyrinoid chromophore, thus allowing for extensive conjugation between the two π systems.[18] This, and the two conjugated ketone functionalities, rationalize the unusual UV−vis spectra of indaphyrins ($\lambda_{\text{max-absorption}} = 810$ nm) when compared to those of porphyrins ($\lambda_{\text{max-absorption}} \sim 650$ nm).[18] Now, the question arises whether the Pt(II) complexes of indaphyrin, **5**, can be prepared, whether they are emissive in the NIR, and whether they can be used as oxygen sensors.

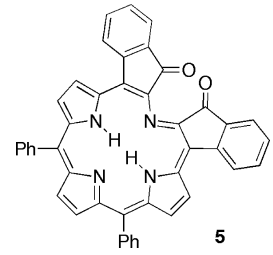

In unrelated studies, we, and others, reported that *meso*-thienyl-porphyrins and corroles possess red-shifted electronic spectra.[19,20] This observation was attributed to the smaller ring size of thiophenes compared to that of phenyl groups, which allows for their greater degree of coplanarity with the porphyrin chromophore. This prompts the question of whether *meso*-thienyl substitution and an indaphyrin-type linkage can be combined to achieve a bathochromic shift in the as-yet unknown *meso*-thienylporphyrin-derived thiaindaphyrins, and their Pt(II) complexes, as compared to their phenyl analogues.

This contribution will demonstrate that these questions can largely be answered in the affirmative. We report here on the preparation, photophysical characteristics, and oxygen-sensing abilities of the Pt(II) complexes of indaphyrin and thiaindaphyrin, **5Pt** and **10Pt**, respectively. We will also report the X-ray single-crystal structure of [*meso*-phenylindaphyrinato]Pt(II) (**5Pt**), the first structural characterization of any indaphyrin, proving their predicted highly ruffled chromophore structure.

(12) Papkovsky, D. B.; Ponomarev, G. V.; Trettnak, W.; O'Leary, P. *Anal. Chem.* **1995**, *67*, 4112–17.
(13) (a) Rogers, J. E.; Nguyen, K. A.; Hufnagle, D. C.; McLean, D. G.; Su, W.; Gossett, K. M.; Burke, A. R.; Vinogradov, S. A.; Pachter, R.; Fleitz, P. A. *J. Phys. Chem. A* **2003**, *107*, 11331–11339. (b) Rozhkov, V. V.; Khajehpour, M.; Vinogradov, S. A. *Inorg. Chem.* **2003**, *42*, 4253–4255. (c) Rietveld, I. B.; Kim, E.; Vinogradov, S. A. *Tetrahedron* **2003**, *59*, 3821–3831.
(14) König, K. *J. Microscopy* **2000**, *200*, 83–104.
(15) Finikova, O. S.; Cheprakov, A. V.; Vinogradov, S. A. *J. Org. Chem.* **2005**, *70*, 9562–9572.
(16) Won, D.-H.; Toganoh, M.; Terada, Y.; Fukatsu, S.; Uno, H.; Furuta, H. *Angew. Chem., Int. Ed.* **2008**, *47*, 5438–5441.
(17) McCarthy, J. R.; Hyland, M. A.; Brückner, C. *Chem. Commun.* **2003**, 1738–1739.
(18) McCarthy, J. R.; Hyland, M. A.; Brückner, C. *Org. Biomol. Chem.* **2004**, *2*, 1484–1491.
(19) Brückner, C.; Foss, P. C. D.; Sullivan, J. O.; Pelto, R.; Zeller, M.; Birge, R. R.; Crundwell, G. *Phys. Chem. Chem. Phys.* **2006**, *8*, 2402–2412.
(20) (a) Bhyrappa, P.; Bhavana, P. *Chem. Phys. Lett.* **2001**, *349*, 399–404. (b) Gupta, I.; Hung, C.-H.; Ravikanth, M *Eur. J. Org. Chem.* **2003**, 4392–4400. (c) Friedlein, R.; Kieseritzky, F. v.; Braun, S.; Linde, C.; Osikowicz, W.; Hellberg, J.; Salaneck, W. R. *Chem. Comm.* **2005**, *15*, 1974–1976. (d) Gupta, I.; Ravikant, M. J. *Photochem. Photobiol. A* **2005**, *177*, 156–163. (e) Bhyrappa, P.; Sankar, M.; Varghese, B.; Bhavana, P. J. *Chem. Sci.* **2006**, *118*, 393–397. (f) Eu, S.; Hayashi, S.; Umeyama, T.; Oguro, A.; Kawasaki, M.; Kadota, N.; Matano, Y.; Imahori, H. *J. Phys. Chem. C* **2007**, *111*, 3528–3537. (g) Maiti, N.; Lee, J.; Kwon, S. J.; Kwak, J.; Do, Y.; Churchill, D. G. *Polyhedron* **2006**, *25*, 1519–1530.

Experimental Section

Instruments and Materials—Synthesis. All solvents and reagents were used as received. *meso*-Tetraphenylporphyrin (**1**),[21] diolchlorin (**7**),[22] free-base indaphyrin (**5**),[18] and *meso*-tetra(5′-methylthien-2′-yl)porphyrin (**6**)[19] were prepared as described before. The analytical thin-layer chromatography (TLC) plates (aluminum-backed, silica gel 60, 250 μm thickness), preparative TLC plates (20 × 20 cm, glass-backed, silica gel 60, 500 or 1000 μm thickness), and flash column silica gel (standard grade, 60 Å, 32−63 μm) used were provided by Sorbent Technologies, Atlanta, Georgia. ^{1}H and ^{13}C NMR spectra were recorded on a Bruker DRX400 spectrometer. The NMR spectra are expressed on the δ scale and were referenced to residual solvent peaks or internal Me_4Si (for copies of the NMR spectra, see the Supporting Information). IR spectra were recorded on a Thermo Nicolet Nexus 670 spectrometer. Mass spectra were provided by the Mass Spectrometry Facilities at the Department of Chemistry, University of Connecticut or the Department of Chemistry and Biochemistry, University of Notre Dame.

Instruments and Materials—Photophysical Characterizations. UV−vis spectra were recorded on a Cary 50 spectrophotometer and the fluorescence spectra on a Cary Eclipse spectrofluorometer (both Varian Inc.). NIR emission spectra were recorded, at 77 K, of samples dissolved in the solvents specified and contained in 5-mm-diameter Pyrex NMR tubes using a modified SPEX Fluorolog 2 spectrometer (J. Y. Horiba, Edison, NJ), equipped with a liquid-nitrogen-cooled Ge diode detector (EO817L; North Coast Scientific Corp.). A 450 W Xe lamp (Osram), in conjunction with a double-grating monochromator, served as the excitation source. The emission spectra reported were not corrected for the wavelength-dependent sensitivity of the detector.

Phosphorescence lifetimes were measured at 77 K using the pulses from a Lambda Physik dye laser (FL3002; Laser dye: Stilbene 3), which was pumped with a Lambda Physik Excimer laser (Lextra). The phosphorescence was collected and isolated using lenses and monochromators (H10 for visual spectral range and 1681B for NIR spectral range; Jobin-Yvon Inc.) and focused into Hamamatsu photomultiplier tubes (PMT; R928 for visual spectral range and H9170-45 for NIR spectral range). The photocurrent from the PMT was amplified (SR 560, Stanford Research Systems) and stored on a digital oscilloscope (TDS 360, Tektronix).

Oxygen-Sensing Experiments. Complex **5Pt** (5 mg) was dissolved in a solution of silicon-polycarbonate LR 3320 (500 mg, General Electric, Fairfield, CT) in CH_2Cl_2 (20 mL). The sensor film was cast and tested following a standard procedure.[23,24] In an alternative approach, the PtDPI was dispensed directly onto 1 × 2 cm TLC plates (500 μm silica on glass).

X-Ray Diffractometry of 5Pt.[25] A dark green needle-shaped crystal of **5Pt** of the approximate dimensions 0.43 × 0.12 × 0.09 mm was obtained by the slow evaporation of a CH_2Cl_2/CH_3CN solution. Diffraction data were collected on a Bruker AXS SMART APEX CCD diffractometer at 100(2) K using monochromatic Mo Kα radiation with the Ω scan technique in the range from θ = 1.43 to 28.28°; the limiting indices were $-11 \le h \le 11$, $-17 \le k \le 16$, and $-19 \le l \le 19$. A total of 16 206 reflections were collected, with 7670 independent reflections (R_{int} = 0.0188), completeness to θ = 28.28°, 99.6%. The SADABS multiscan absorption correction was applied.[25a] The data were collected using SMART,[25b] and the data integration and unit cell determination were made using SAINT+.[25a] The structure was solved by direct methods and refined by full-matrix least-squares against F^2 using SHELXTL.[25c] The goodness-of-fit on F^2 was 1.074; the largest differential peak and hole were 1.879 and −0.940 e·Å^{-3}. A full-matrix refinement method on the least-squares on F^2 was applied. Data, restraints, and parameters were 7670, 0, and 460. Non-hydrogen atoms were refined with anisotropic displacement parameters. All hydrogen atoms were placed in calculated positions and were isotropically refined with a displacement parameter of 1.2 times that of the adjacent carbon atom. The refinement converged satisfactorily. The crystal structure and refinement data for **5Pt** are summarized in Table 1. Selected bond lengths and distances are tabulated in Table 2.

Table 1. Selected Crystallographic Data and Structure Refinement Details for **5Pt**[a]

empirical formula	$C_{44}H_{24}N_4O_2Pt$
fw, g/mol	835.76
space group	$P\bar{1}$ (No. 2)
λ, Å	0.71073
a, Å	8.8735(4)
b, Å	12.9285(6)
c, Å	14.3297(6)
α, deg	88.7850(10)
β, deg	82.2480(10)
γ, deg	72.4220(10)
volume, Å^3	1552.50(12)
d_{calcd}, g/cm^3	1.788
Z	2
μ, mm^{-1}	4.569
transmission coeff	0.663, 0.377
final R indices [$I > 2\sigma(I)$]	R1 = 0.0247, wR2 = 0.0628
R indices (all data)	R1 = 0.0260, wR2 = 0.0635

[a] The weighted R factor wR and goodness of fit are based on F^2, conventional R factor R is based on F, with F set to zero for negative F^2. The threshold expression of $F^2 > 2\sigma(F^2)$ is used only for calculating R factors.

[*meso*-Diphenylindaphyrinato]Pt(II) (5Pt). To a solution of free-base indaphyrin, **5** (59 mg, 0.09 mmol), in PhCN (15 mL) was added bis-2,4-pentanedionate [Pt(acac)$_2$] (108 mg, 0.28 mmol, 3 equiv). The reaction mixture was refluxed and monitored by TLC and UV−vis until the starting material was exhausted (5 h). The solvent was removed in vacuo. The mixture was passed through a plug of silica with CH_2Cl_2. The residue was further purified by preparative TLC (silica-CH_2Cl_2/*n*-hexane 4:1) and recrystallized from $CHCl_3$/EtOH to give **5Pt** as a purple solid (50 mg, 0.06 mmol, 65%). R_f (silica- CH_2Cl_2): 0.42. UV−vis (CH_2Cl_2) λ_{max} (log ε): 391 (3.86), 462 (sh), 495 (sh), 525 (4.16), 632 (3.54), 677 (3.48) nm. IR (neat) ν_{max}: 1706 (C═O) cm^{-1}. ^{1}H NMR (400 MHz, $CDCl_3$): 7.37 (t, ^3J = 7.6 Hz, 1H), 7.50−7.60 (br s, 1H), 7.67 (t, ^3J = 7.6 Hz, 2H), 7.75 (br t, 3H), 7.90 (d, ^3J = 7.6 Hz, 1H), 8.26 (d, ^3J = 7.6 Hz, 1H), 8.43 (s, 1H), 8.66 (d, ^3J = 5.2 Hz, 1H), 9.25 (d, ^3J = 5.2 Hz, 1H) ppm. ^{13}C NMR (100 MHz, $CDCl_3$): 117.2, 125.0, 126.2, 126.7, 127.0, 128.3, 129.0, 129.1, 131.4, 132.3, 136.3, 136.4, 137.1, 137.9, 138.6, 140.1, 146.2, 187.2 ppm. MS (ESI$^+$, 100% CH_3CN): *m/z* 835 (M^+). HRMS (EI, 30 eV): *m/z* calcd for $C_{44}H_{25}N_4O_2Pt$: (M^+) 835.1547. Found: 835.1546. Anal. calcd for $C_{44}H_{24}N_4O_2Pt$: C, 63.23; H, 2.89; N, 6.70. Found: C, 63.19; H, 2.88; N, 6.68.

(21) Adler, A. D.; Longo, F. R.; Finarelli, J. D.; Goldmacher, J.; Assour, J.; Korsakoff, L. *J. Org. Chem.* **1967**, *32*, 476.

(22) Brückner, C.; Rettig, S. J.; Dolphin, D. *J. Org. Chem.* **1998**, *63*, 2094–2098.

(23) Khalil, G.; Gouterman, M.; Ching, S.; Costin, C.; Coyle, L.; Gouin, S.; Green, E.; Sadilek, M.; Wan, R.; Yearyean, J.; Zelelow, B. *J. Porphyrins Phthalocyanines* **2002**, *6*, 135–145.

(24) Gamal, K. E.; Thompson, E. K.; Gouterman, M.; Callis, J. B.; Dalton, L. R.; Turro, N. J.; Jockusch, S. *Chem. Phys. Lett.* **2007**, *435*, 45–49.

(25) (a) *Bruker Advanced X-ray Solutions SAINT*, version 6.45; Bruker AXS Inc.: Madison, WI, 1997−2003. (b) *Bruker Advanced X-ray Solutions SMART for WNT/2000*, version 5.628; Bruker AXS Inc.: Madison, WI, 1997− 2002. (c) *Bruker Advanced X-ray Solutions SHELXTL*, version 6.10; Bruker AXS Inc., Madison, WI, 2000.

Table 2. Select Bond Lengths and Angles for **5Pt**[a]

bond	length [Å]	bond	angle [deg]
C(1)−N(1)	1.360(3)	N(1)−C(1)−C(9)	126.9(2)
C(1)−C(9)	1.389(4)	C(9)−C(1)−C(2)	108.8(2)
C(1)−C(2)	1.504(4)	O(1)−C(2)−C(3)	126.9(3)
C(2)−O(1)	1.208(3)	O(1)−C(2)−C(1)	127.5(3)
C(2)−C(3)	1.486(4)	C(3)−C(2)−C(1)	105.3(2)
C(3)−C(8)	1.409(4)	C(1)−C(9)−C(10)	124.6(2)
C(8)−C(9)	1.489(4)	C(1)−C(9)−C(8)	108.6(2)
C(9)−C(10)	1.392(4)	C(10)−C(9)−C(8)	126.8(2)
C(10)−N(2)	1.384(3)	N(2)−C(10)−C(9)	122.9(2)
C(10)−C(11)	1.437(4)	N(2)−C(10)−C(11)	109.1(2)
C(11)−C(12)	1.354(4)	C(9)−C(10)−C(11)	127.9(2)
C(12)−C(13)	1.439(4)	C(12)−C(11)−C(10)	107.6(2)
C(13)−N(2)	1.383(3)	C(11)−C(12)−C(13)	107.4(2)
C(13)−C(14)	1.402(4)	N(2)−C(13)−C(14)	125.2(2)
C(14)−C(15)	1.402(4)	N(2)−C(13)−C(12)	109.1(2)
C(15)−N(3)	1.387(3)	C(14)−C(13)−C(12)	125.2(2)
C(15)−C(16)	1.431(4)	C(13)−C(14)−C(15)	123.6(2)
C(16)−C(17)	1.359(4)	N(3)−C(15)−C(14)	125.3(2)
N(1)−Pt(1)	2.004(2)	N(3)−C(15)−C(16)	109.0(2)
N(2)−Pt(1)	2.002(2)	C(14)−C(15)−C(16)	125.7(2)
N(3)−Pt(1)	2.000(2)	C(17)−C(16)−C(15)	107.9(2)
N(4)−Pt(1)	2.007(2)	C(16)−C(17)−C(18)	107.1(2)
		N(3)−C(18)−C(19)	125.6(2)
		N(3)−C(18)−C(17)	109.4(2)
		C(1)−N(1)−C(32)	115.5(2)
		C(13)−N(2)−C(10)	106.7(2)
		C(18)−N(3)−C(15)	106.5(2)
		N(3)−Pt(1)−N(2)	89.67(9)
		N(3)−Pt(1)−N(1)	179.76(8)
		N(2)−Pt(1)−N(1)	90.29(9)
		N(2)−Pt(1)−N(4)	179.24(8)

[a] Each molecule of **5Pt** is pseudo-2-fold symmetric; hence, only half the data are presented. For a full data set, see the Supporting Information.

***meso*-Tetra(5′-methylthien-2′-yl)-2,3-cis-dihydroxy-2,3-chlorin (8). Caution!** *The synthesis requires a rotary evaporator in a well-ventilated fume hood as the particularly volatile and toxic reagents OsO_4 and H_2S are used!* A solution of *meso*-tetra(5′-methylthien-2′-yl)porphyrin, **6** (500 mg, 0.72 mmol), and OsO_4 (250 mg, 0.98 mmol) in EtOH-stabilized chloroform/50% pyridine (120 mL) was stirred at room temperature for 4 days. The reaction was quenched, at ambient conditions, by purging with gaseous H_2S for 5 min, followed by stirring for an additional 30 min. The solution was filtered through a plug of Celite. The filtrate was evaporated to dryness by rotary evaporation, and the residue was separated by column chromatography (silica-gel gradient of $CHCl_3$/MeOH). Two fractions were isolated: the first was recovered purple porphyrin **6** (224 mg, 45%; $R_f = 0.90$ (silica-$CHCl_3$)), and the second fraction was the purple-brown chlorin **8** (193 mg, 26% yield). $R_f = 0.22$ (silica-$CHCl_3$). UV−vis ($CHCl_3$) λ_{max} (log ε): 428 (5.21), 528 (4.13), 560 (4.18), 607 (3.92), 660 (4.39) nm. ^{1}H NMR (400 MHz, $CDCl_3$) δ: −1.63 (s, exchangeable with D_2O, 1H), 2.75 (s, 3H), 2.78 (s, 3H), 3.55 (s, exchangeable with D_2O, 1H), 6.53 (s, 1H), 7.08−7.11 (m, 2H), 7.51 (d, $J = 3.2$ Hz, 1H), 7.60 (d, $J = 3.2$ Hz, 1H), 8.59 (d, $J = 4.8$ Hz, 1H), 8.74 (s, 1H), 8.94 (d, $J = 4.8$ Hz, 1H) ppm. ^{13}C NMR (100 MHz, $CDCl_3$) δ: 15.6, 15.7, 74.3, 105.5, 116.2, 124.3, 124.7, 125.0, 128.4, 132.1, 132.7, 133.2, 136.6, 139.4, 140.1, 141.9, 142.1, 142.6, 154.2, 163.2 ppm. HRMS (ESI+) *m*/*z* calcd for $C_{40}H_{33}N_4O_2S_4$: $(M + H)^+$ 729.1481. Found: 729.1488.

***meso*-Tri(5′-methylthien-2′-yl)-1-formylthiaindaphyrin (9).** A solution of diol **8** (100 mg, 0.14 mmol) and excess $NaIO_4$ heterogenized on silica gel[18] (1.0 g) in $CHCl_3$ (25 mL) was stirred at room temperature overnight. The oxidant was removed by filtration (glass frit M), and the filtrate was evaporated to dryness by rotary evaporation. The residue was separated by column chromatography (silica gel-$CHCl_3$). The orange compound **9** (70 mg, 70% yield) was isolated. $R_f = 0.55$ (silica-$CHCl_3$). UV−vis ($CHCl_3$) λ_{max} (log ε): 444 (4.77), 478 (4.71), 722 (4.16) nm. IR (neat) ν_{max}: 1648, 1691 (C═O) cm^{-1}. ^{1}H NMR (400 MHz, $CDCl_3$) δ: 2.57 (s, 3H), 2.70 (s, 3H), 2.72 (s, 6H), 3.34 (br s, exchangeable with D_2O, 2H), 6.89 (s, 1H), 6.99 (d, $J = 2.8$ Hz, 1H), 7.03 (d, $J = 2.7$ Hz, 1H), 7.09 (d, $J = 2.4$ Hz, 1H), 7.26 (signal hidden under $CHCl_3$ signal, as seen in H,H-COSY), 7.30 (d, $J = 2.8$ Hz, 1H), 7.45 (d, $J = 2.7$ Hz, 1H), 8.08 (d, $J = 4.6$ Hz, 1H), 8.17 (d, $J = 4.6$ Hz, 1H), 8.24 (brs, 2H), 8.32 (d, $J = 4.9$ Hz, 1H), 8.36 (d, $J = 4.9$ Hz, 1H), 9.28 (s, 1H) ppm. ^{13}C NMR (100 MHz, $CDCl_3$) δ: 15.5, 15.6, 15.9, 16.0, 110.7, 119.6, 120.5, 121.1, 124.2, 124.4, 125.0, 125.1, 125.2, 126.3, 131.4, 131.6, 132.2, 133.4, 134.1, 134.8, 135.4, 137.2, 137.8, 138.2, 139.0, 140.4, 142.4, 143.7, 144.9, 154.0, 154.4, 161.3, 165.3, 181.3, 185.0 ppm. HRMS (ESI+) *m*/*z* calcd for $C_{40}H_{29}N_4O_2S_4$: $(M + H)^+$ 725.1168. Found: 725.1163.

***meso*-Di(5′-methylthien-2′-yl)thiaindaphyrin (10).** Monoaldehyde **9** (100 mg, 0.14 mmol) was dissolved in 2%TFA/CH_2Cl_2 (25 mL). The solution was stirred at ambient temperature overnight and then was washed twice with aqueous $NaHCO_3$ and once with H_2O. The solution was dried over anhydrous Na_2SO_4 and evaporated to dryness. The residue was separated by column chromatography (silica gel-$CHCl_3$). The purple compound **10** (33 mg, 33% yield) was isolated. $R_f = 0.65$ (silica-$CHCl_3$). UV−vis ($CHCl_3$) λ_{max} (log ε): 432 (4.54), 570 (4.31) nm. IR (neat) ν_{max}: 1678, 1694 (C═O) cm^{-1}. ^{1}H NMR (400 MHz, $CDCl_3$) δ: 1.16 (s, 1H), 2.55 (s, 3H), 2.72 (s, 3H), 6.88 (s, 1H), 7.01 (d, $J = 3.0$ Hz, 1H), 7.39 (d, $J = 3.0$ Hz, 1H), 8.35 (s, 1H), 8.61 (d, $J = 4.7$ Hz, 1H), 8.64 (d, $J = 4.7$ Hz, 1H). ^{13}C NMR (100 MHz, $CDCl_3$) δ: 15.5, 15.9, 114.6, 116.3, 119.7, 122.6, 124.8, 129.2, 131.4, 132.9, 133.9, 134.4, 138.7, 138.8, 142.7, 144.9, 148.2, 157.2, 161.8, 183.3 ppm. HRMS (ESI+) *m*/*z* calcd for $C_{40}H_{27}N_4O_2S_4$ $(M + H)^+$ 723.1011. Found: 723.1003. Anal. calcd for $C_{40}H_{26}N_4O_2S_4 \cdot 1/2CHCl_3$: C, 62.16; H, 3.41; N, 6.80. Found: C, 62.09; H, 3.38; N, 6.70.

[*meso*-Di(5′-methylthien-2′-yl)thiaindaphyrinato]Pt(II) (10Pt). A solution of **10** (40 mg, 6 mmol) and [Pt(acac)$_2$] (65 mg, 3 equiv) in PhCN (10 mL) was heated until, using TLC and UV−vis reaction control, the starting material was exhausted (either for 8 h at ∼160 °C or 5 h at reflux temperature). The solvent was evaporated under high vacuum conditions, and the residue was separated by column chromatography (silica gel-$CHCl_3$). The red compound **10Pt** (31 mg, 61% yield) was isolated. $R_f = 0.42$ (silica-$CHCl_3$). UV−vis ($CHCl_3$) λ_{max} (log ε): 414 (4.02), 529 (4.23), 648 (3.62) nm. IR (neat) ν_{max}: 1680, 1696 (C═O) cm^{-1}. ^{1}H NMR (400 MHz, $CDCl_3$): δ 2.59 (s, 3H), 2.75 (s, 3H), 6.90 (br s, 1H), 7.04 (d, $^3J = 3.6$ Hz, 1H), 7.41 (d, $^3J = 4.0$ Hz, 1H), 8.39 (s, 1H), 8.64 (d, $^3J = 4.0$ Hz, 1H), 8.67 (d, $^3J = 4.0$ Hz, 1H) ppm. ^{13}C NMR (100 MHz, $CDCl_3$) δ: 15.5, 16.0, 114.5, 116.6, 119.8, 122.6, 124.9, 129.2, 131.6, 133.0, 133.7, 134.4, 138.8, 138.9, 142.9, 144.9, 148.3, 161.8, 183.2 ppm. MS (ESI$^+$, 100% CH_3CN): *m*/*z* 915 (M^+). HRMS (EI, 30 eV) *m*/*z* calcd for $C_{40}H_{24}N_4O_2PtS_4$: (M^+) 915.0430. Found: 915.0418.

Results and Discussion

Synthesis of 5Pt, the Pt(II) complex of indaphyrin 5. The synthesis of diphenylindaphyrin **5** proceeded along the pathway described previously (Scheme 1).[18] Thus, dihydroxylation of *meso*-tetraphenylporphyrin **1**[22] was followed by the oxidative diol cleavage of diol **7**. The resulting bisaldehyde underwent, in situ, an acid-catalyzed intramolecular Friedel−Crafts alkylation with concomitant air oxidation. Insertion of Pt(II) into porphyrins generally requires the heating of a Pt(II) salt, such as the acetate, chloride, or acetyl acetonate, in benzonitrile at reflux temperatures (191

Scheme 1[a]

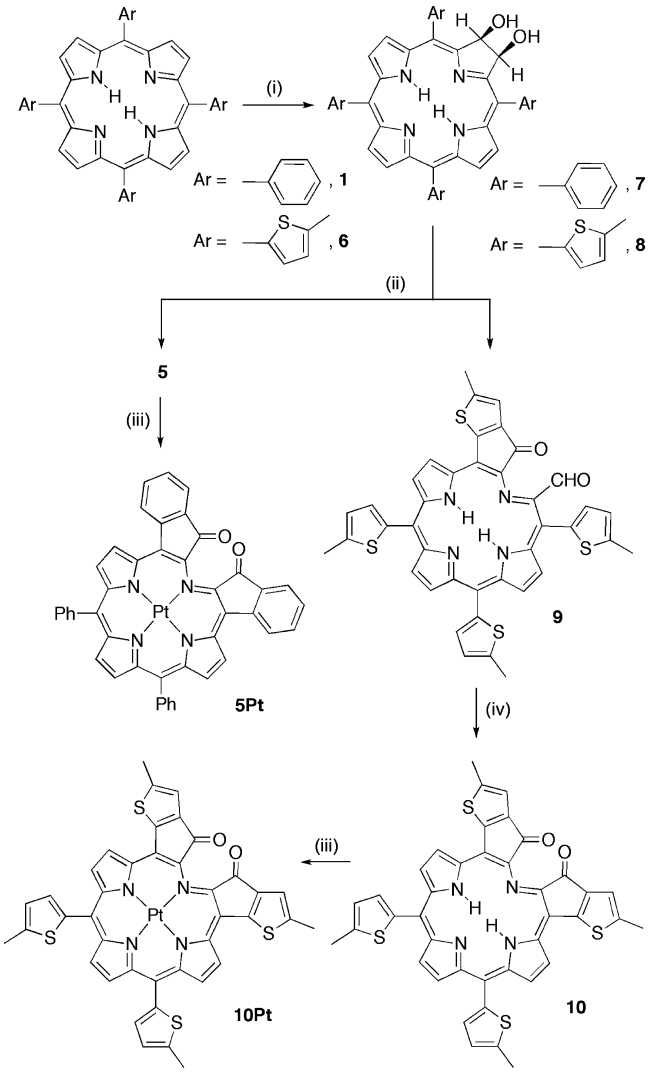

[a] Reaction conditions: (i)[22] 1. OsO_4/pyridine, $CHCl_3$ (EtOH-stabilized), ambient temperature, 4 d; 2. H_2S; 3. chromatography. (ii)[18] $NaIO_4$ on silica gel, $CHCl_3$, ambient temperature, air. (iii) [Pt(acac)$_2$], PhCN, reflux, 5h. (iv) 2% TFA in CH_2Cl_2, ambient temperature, air.

°C) for extended periods of time (typically 12−24 h).[26,27] Appreciable Pt(II) insertion into indaphyrin **5** already takes place in benzonitrile at 140−160 °C. At reflux temperatures, the reaction is completed within 3−5 h. We attribute this to the much greater conformational flexibility of the indaphyrin chromophore as compared to that of a porphyrin. Chromatography, followed by recrystallization, produced Pt(II) indaphyrin **5Pt** in good yields.

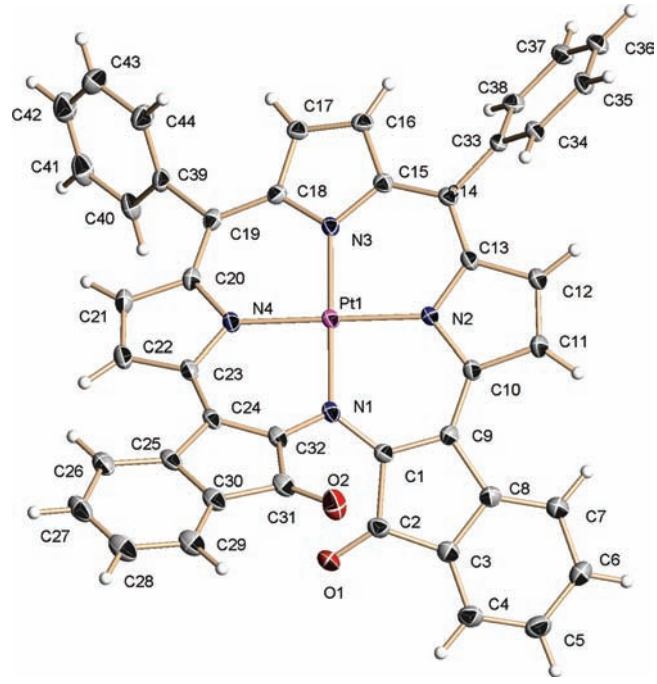

Figure 1. ORTEP representation (50% ellipsoids) and numbering scheme of the molecular structure of **5Pt**.

The spectroscopic and analytical data were all consistent with the structure of **5Pt**. In particular, its ^{1}H and ^{13}C NMR spectra were very similar to those of free-base **5**, an indication that the insertion of Pt(II) did not lead to dramatic structural changes. As detailed below, a single-crystal structure analysis of **5Pt** confirms its connectivity and highlights its conformation. The optical properties of all chromophores synthesized are discussed below.

Metal complexes of indaphyrins were described before.[18] However, the Ni(II) complexes of indaphyrins are unstable and form ring-opened products within days in solution, though the larger ions Cu(II) and Zn(II) form stable indaphyrinato complexes.[18] Complex **5Pt** is stable in solution for days and as a solid for at least 2 years.

X-Ray Structure of 5Pt. Figures 1 and 2 and Table 2 show the results of a single-crystal diffractometry analysis of crystals of **5Pt**. The structure, the first X-ray structure of any indaphyrin, confirms the spectroscopically derived connectivity of **5Pt**. It shows the significant degree of ruffling of the chromophore, with a root-mean-square (rms) deviation from the average plane of the $C_{20}N_4Pt$ core of 0.448 Å.[28] In comparison, an example of a severely nonplanar [morpholinochlorinato]Ni(II) complex shows an rms deviation from planarity of its $C_{20}N_4Ni$ core of 0.468Å.[22,29] As a result of the ruffling, a 46° dihedral angle between the mean planes of the two indanone moieties is observed.

The ruffling observed in Ni(II) porphyrins is caused by the presence of the small metal ion.[29−31] The ruffling distortion mode allows for a shortening of the N−Ni bonds without any deviation of the nitrogens from a square-planar coordination sphere around the central metal. Indeed, in **5Pt**, the N_4Pt bond lengths and angles are also nearly perfectly square-planar (deviations from the $C_{20}N_4Pt$ mean plane lie between 0.006(2) Å for N1 and 0.148(2) Å for N2). In

(26) Buchler, J. W. In *The Porphyrins*; Dolphin, D., Ed.; Academic Press: New York, 1978; Vol. *1*, p 389−483.
(27) Dean, M. L.; Schmink, J. R.; Leadbeater, N. E.; Brückner, C. *Dalton Trans.* **2008**, 1341–1345.
(28) The contribution of the various non-planar conformational modes to the overall conformation of a porphyrin can be computed using a normal coordinate structural analysis, see: Shelnutt, J. A. In *The Porphyrin Handbook*; Kadish, K. M., Smith, K. M., Guilard, R., Eds.; Academic Press: San Diego, CA, 2000; Vol. *7*, pp 167−224. The different macrocycle connectivity of indaphyrins, however, does not allow their analysis along any porphyrin lowest-energy frequency mode using the NSD Engine (http://jasheln.unm.edu/jasheln/content/nsd/NSDengine/start.htm, accessed Mar 2009).

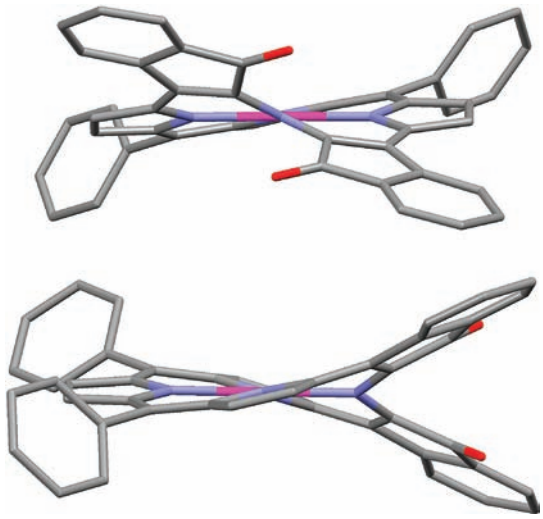

Figure 2. Front view (top) along the N(1)−Pt(1)−N(3) bond axis and (bottom) side view along the N(4)−Pt(1)−N(2) bond axis of the molecular structure of **5Pt**. Hydrogen atoms are omitted for clarity.

contrast to the Ni(II) porphyrins, however, the distortion is intrinsic to the indaphyrin ligand. This is because the conformation of the ligand in **5Pt** is, albeit slightly more pronounced, very similar to that computed for free-base **5** (rms deviation of the $C_{20}N_4$ core from planarity was computed to be 0.39 Å).[18] Interestingly, the observed N−Pt bond lengths (average of 2.003(2) Å) are identical to those observed in the slightly ruffled [porphyrinato]Pt(II) complexes (2.005 Å in **1Pt** at 295 K).[32]

The cleavage of the pyrrole and fusion of two indanone units into the macrocycle results in a significant dissymmetry of the bond lengths and angles within the porphyrinoid macrocycle (Table 2). For instance, the $N(1)^{imine}-C(1)^{indanone}$ and the $C(1)^{indanone}-C(9)^{indanone}$ bond lengths are significantly shorter (1.360(3) and 1.389(4) Å, respectively) compared to the corresponding and unusually long $N(2\text{ or }3)^{pyrrole}-C(11/13\text{ or }15/18)^{pyrrole}$ (average of 1.385(3) Å) and $C(13/15)^{pyrrole}-C(14)^{meso}$ bond lengths (1.402(4) Å), respectively. The corresponding bond lengths in metalloporphyrin **1Pt** lie, with an average $N-C^{\alpha}$ length of 1.376 Å and an average $C^{\alpha}-C^{meso}$ length of 1.388 Å, between the two extreme values observed in **5Pt**. The C−N−C bond angles within the pyrrole units are with 107° within the range expected in a porphyrin, whereas the bond angle of the imine-type linkage between the indanone units is widened to 115°.

The crystal is composed of offset columns of π-stacked pairs of **5Pt** that are held together by $\pi-\pi$ interactions between *meso*-phenyl groups. No major channels or cavities are discernible. Complex **5Pt** is chiral and crystallizes as a racemate in the nonchiral space group $P\bar{1}$.

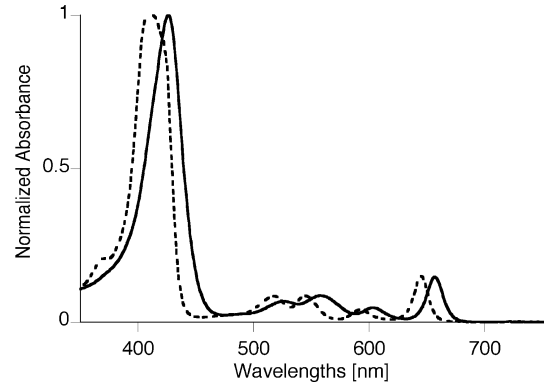

Figure 3. Normalized UV−vis spectra of **7** (broken trace) and **8** (solid trace) in CH_2Cl_2 + 0.1% of Et_3N. For the spectra of these species in the presence of TFA, see the Supporting Information.

Synthesis of the Dithienylthiaindaphyrin 10 and Its Pt(II) Complex 10Pt. The synthetic methodology toward indaphyrin **5** is perceivably transferable to any *meso*-arylporphyrin with an ortho position on the *meso*-aryl group that is susceptible to electrophilic aromatic substitution, including also *meso*-thien-2-ylporphyrin, **6** (Scheme 1). Thus, osmylation/reduction of the *meso*-tetra(4-methyl-thien-2-yl)porphyrin,[33] **6**, resulted in the formation of the corresponding diol chlorin **8**. Its HRMS (ESI+, m/z = 729.1488 for $[M + H]^+$) spectrum confirms its composition ($C_{40}H_{33}N_4O_2S_4$), and diagnostic peaks in the ^1H and ^{13}C NMR spectrum confirm its structure. Moreover, the UV−vis spectrum of **8** is a typical chlorin spectrum, with λ_{max} at 658 nm the most intense of all side bands. It is, as expected, based on the comparison of thienylporphyrins with phenylporphyrins,[19] ~12 nm bathochromically shifted compared to that of *meso*-phenyl-based chlorin **7** (Figure 3).[22,34]

Oxidative diol cleavage of diol **8** using $NaIO_4$ heterogenized on silica gel results in the formation of a putative bisaldehyde intermediate that, analogous to the reactivity of its *meso*-phenyl analogue,[17,18] spontaneously undergoes a Friedel−Crafts alkylation with concomitant oxidation to form monothiaindanone monoaldehyde **9**. It is identified by the characteristic loss of symmetry in the ^1H and ^{13}C NMR spectra; an ESI+ HRMS indicative of the expected composition for MH^+ ($C_{40}H_{29}N_4O_2S_4$); and the appearance of one aldehyde signal in the ^1H NMR (9.28 ppm, s, 1H) and two carbonyl signals in the ^{13}C NMR (181.1, 185.0 ppm) and IR (ν = 1691, 1648 cm^{-1}) spectra. Product **9** possesses, however, only limited stability in solution. Using 2% TFA in CH_2Cl_2, this orange product is converted to a brown-purple and slightly less polar product that could be identified as the *meso*-di(5′-methylthien-2-yl)-substituted thiaindaphyrin **10**. Its HR-MS spectrum indicates the loss of two hydrogens compared to the composition of its precursor **9**. Its ^1H and ^{13}C NMR spectra suggest a molecule of 2-fold symmetry with diagnostic signals for the presence of an ortho-linked

(29) Brückner, C.; Hyland, M. A.; Sternberg, E. D.; MacAlpine, J.; Rettig, S. J.; Patrick, B. O.; Dolphin, D. *Inorg. Chim. Acta* **2005**, *358*, 2943–2953.
(30) Kratky, C.; Waditschatka, R.; Angst, C.; Johansen, J. E.; Plaquevent, J. C.; Schreiber, J.; Eschenmoser, A. *Helv. Chim. Acta* **1985**, *68*, 1313–1337.
(31) Barkigia, K. M.; Berber, M. D.; Fajer, J.; Medforth, C. J.; Renner, M. W.; Smith, K. M. *J. Am. Chem. Soc.* **1990**, *112*, 8851–8857.
(32) Hazell, A *Acta Crystallogr., Sect. C: Cryst. Struct. Commun.* **1984**, *40*, 751. CSD code: CEZKEX.
(33) This particular thiophen-2-yl porphyrin derivative was chosen, as it was characterized by a significantly red-shifted UV−vis spectrum compared to the corresponding non-methylated compound, see ref 19.
(34) Interestingly, the unique acid−base dependency of the optical properties of chlorin 8 vs chlorin 7 is similar to the shifts observed for the porphyrins, see ref 19. The spectra are shown in the Supporting Information.

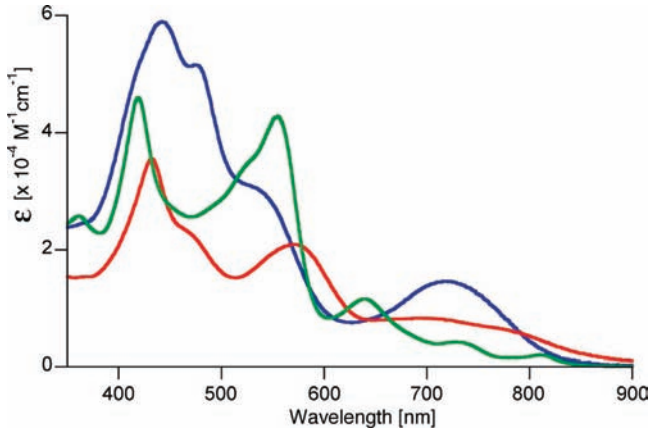

Figure 4. UV−vis spectra of **5** (green trace), **9** (blue trace), and **10** (red trace) in CH_2Cl_2 + 0.1% of Et_3N.

aryl group,[18] only three types of thienyl β-protons, and one type of ketone functionality (183.3 ppm in the ^{13}C NMR). Further, a comparatively high-field-shifted signal assigned to the NH protons can be discerned (1.16 ppm, br s, 1H), another characteristic of indaphyrins that is likely a reflection of the great distortion from planarity in these porphyrinoids.[18] Taken together, the spectroscopic data confirm the structure of **10**. It is interesting to note that the formation of a thiaindanone[35] moiety in the target compound **10** appears to be similarly facile as in the phenyl derivative **5**, despite the fact that the steric requirements of forming the indanone moiety (one five- and six-membered fused ring) are different from those for the formation of a thiaindanone unit (two fused five-membered rings).

The insertion of Pt(II) into **10** also proceeded smoothly, and **10Pt** could be isolated as a microcrystalline powder in 65% yield. It possesses all of the expected spectroscopic and analytical properties. Aside from the disappearance of the signals for the NH protons, only minor shifts in the ^1H NMR spectrum are observed upon the insertion of Pt(II) into free-base **10**. This is likely a testimony to the preservation of the conformation of the free ligand in its complex. A Pt(II) insertion into thiaindaphyrin monoaldehyde **9** failed due to the instability of the ligand.

Photophysical Properties of 5 and 10, and Their Pt(II) Complexes. The UV−vis spectra of free-base *meso*-tri(thien-2-yl)formylthiaindaphyrin, **9**, and *meso*-di(thien-2-yl)thiaindaphyrin, **10**, in comparison to that of known *meso*-diphenylindaphyrin, **5**,[18] are shown in Figure 4. The spectrum of thienyl derivative **10** is, as hoped for, red-shifted compared to that of the phenyl analogue **5**, though the number and relative intensities of the bands also vary slightly. This is a reflection of the differing π systems of the two chromophores and the differing conformation and conformational flexibility. The relatively broad and far-into-the-red-reaching bands of **5** and **10** allow a prediction for ligand-based emissions in the NIR for their Pt(II) complexes. The spectrum of the formylated "half-thiaindaphyrin" **9** possesses larger extinction coefficients and appears to be more "porphyrin-like", an observation also made for its phenyl analogue.[18]

(35) The formal name for the resulting moiety is cyclopenta[b]thiophen-4-one, also referred to as thiaindanone: Aparajithan, K.; Thompson, A. C.; Sam, J. *J. Heterocycl. Chem.* **1966**, *3*, 466–469.

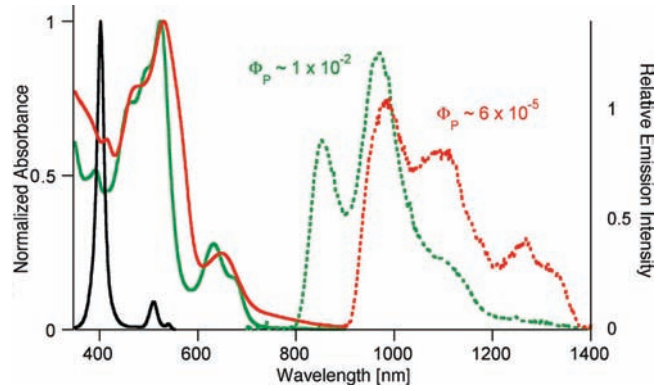

Figure 5. UV−vis absorption spectra (CH_2Cl_2, r.t.) of **1Pt** (solid black trace), **5Pt** (solid green trace), and **10Pt** (solid red trace) in CH_2Cl_2; phosphorescence emission spectra (EtOH glass, 77 K) of **5Pt** (dotted green trace; $\lambda_{excitation}$ = 524 nm) and **10Pt** (dotted red trace; $\lambda_{excitation}$ = 529 nm). The emission spectra were confirmed using excitation emission scans.

Figure 5 shows the absorption spectra of the Pt(II) complexes **5Pt** and **10Pt** in comparison to that of **1Pt**. The main absorption bands of **5Pt** and **10Pt** are a Soret-like band (for **5Pt** at ~ 525 nm; ε = 14 500 M^{-1} cm^{-1}) and two side bands (at 632 and 677 nm, ε = 3500 and 3000 M^{-1} cm^{-1}, respectively) with a vibrational spacing of 1070 cm^{-1}, assuming that the origin of the bands is similar to that of **1Pt**. The absorption spectrum of **5Pt** has little resemblance to that of a platinum porphyrin complex (**1Pt**). It is much broader, spanning almost the entire visible spectral region up to ~680 nm, albeit the extinction coefficients of the bands are only ~10% of those of **1Pt**. A broad absorption spectrum has the advantage that it allows for the use of many readily available excitation light sources. As predicted, the absorption spectrum of **10Pt** is slightly bathochromically shifted compared to that of **5Pt**. Also reflecting the trend seen in the free base thiaindaphyrin, the spectrum of **10Pt** is relatively broad.

Spin−orbit interactions with the coordinated $5d^8$ ion Pt(II) increase the intersystem crossing rate of photoexcited Pt(II) porphyrin, resulting in very high triplet yields.[2] Subsequent phosphorescence emissions are on the nanosecond to microsecond scale. Ideally, the observed lifetimes of the $^3T_1$ state are above ~10 μs, allowing ample opportunity for the quenching of the triplet state by $^3O_2$. In this triplet lifetime regime, high sensitivity with respect to the oxygen-pressure measurement can also be achieved through a time-resolved recording of the luminescence.[36]

The phosphorescence emission spectra of **5Pt** and **10Pt** in EtOH at 77 K are shown in Figure 5. The emission spectra are two-band spectra that are strongly solvochromic (**5Pt**: $\lambda_{max\text{-}emission}$ = 850 and 965 nm in EtOH and $\lambda_{max\text{-}emission}$ = 880 and 995 nm in methylcyclohexane, see Supporting Information) with a minimum Stokes shift of 2880 cm^{-1}. No detectable spectral sharpening was detected for the 10^{-6} M solution of **5Pt** in *n*-octane, a Shopl'skii-type matrix. The emissions around 1000 nm are several hundreds of nanometers red-shifted compared to those observed in Pt porphyrins and related derivatives and are comparable to that of the

(36) Lippitsch, M. E.; Draxler, S.; Kieslinger, D. *Sens. Actuators B* **1997**, *B38*, 96–102.

structurally more complex calyx[6]phyrin Pt_2 complex **4Pt$_2$**.[16] While the phosphorescence quantum yield for the phenyl derivative **5Pt**, at 77 K in an deoxygenated EtOH glass, is ~1%, it is about 3 orders of magnitude less in the thio analogue **10Pt** ($\sim 6 \times 10^{-3}$ %). In comparison, the quantum yield for **1Pt** is near unity, and that of the **2Pt** is 70%.[23] This low quantum yield (and short triplet lifetime, see below) are likely caused by a larger conformational flexibility of the indaphyrin and the conjugated ketone oxygens. Considering the very low reported fluorescence yields for thienylporphyrins, the low emission yield for **10Pt** is not a surprise.[22]

The triplet lifetime of **5Pt** was determined to be a relatively short 2 μs. In comparison, the triplet lifetime for **1Pt** is 120 μs, and that for **2Pt** is 70 μs,[9] while the Pt_2 complexes of calix[6]phyrin are characterized by two-digit nanosecond lifetimes (at r.t.).[16]

Testing of 5Pt as Oxygen Sensor. One notable application of oxygen sensors is in air flow visualization. In this application, also referred to as phosphorescence barometry, a sensor is incorporated into an oxygen-permeable polymer matrix that is applied to a surface. The resulting thin layer serves as a two-dimensional air pressure profile sensor for objects exposed to wind flow.[2,10,11]

The oxygen sensitivity of **5Pt** was first tested by incorporating it into a gas-permeable silicon−polycarbonate copolymer matrix. Disappointingly, no oxygen sensitivity was detected. Subsequently, **5Pt** was dispensed directly onto a silica TLC plate. TLC plates provide a chemically neutral flat surface that is highly reflective, and serves as an open configuration with a highly oxygen-permeable surface. Upon irradiation with light of 520 nm, the oxygen partial pressure dependency of the phosphorescence emission of **5Pt** in the range from 700 to 1400 nm was recorded. In the range from 0 to 100% O_2, the intensity of the emission was quenched by only 15% (see Supporting Information), indicating that this dye is not a practical dye for O_2 sensing. The low sensitivity of **5Pt** towards a variation of [O_2] can likely be attributed to the short phosphorescence lifetime of the Pt(II) indaphyrin.

Summary and Conclusions

The Pt(II) complex of indaphyrin **5**, **5Pt**, forms readily and is stable. Its nonplanar conformation was proven to be most similar to the computed conformation of the free-base ligand **5**. Their *meso*-thienyl analogues, free-base thiaindaphyrin **10** and its Pt(II) complex **10Pt**, can also be formed in acceptable yields. They are the first examples of non-*meso*-phenylporphyrin-derived indaphyrins. Significantly, **5Pt** and **10Pt** possess the expected NIR emission spectra, but their short triplet lifetimes, relatively low emission yields, and impractically low sensitivity of the emission intensity variation with respect to changing oxygen partial pressure render these complexes unsuitable as practical oxygen sensors.

Acknowledgment. We thank Paul Foss for preliminary work on the preparation of **8** and Pedro Daddario for technical assistance. C.B. thanks the National Science Foundation for financial support through grants NSF CHE-0517782 and NSF CMMI-0730826. This work was also supported by the Department of Defense Multi-Disciplinary University Research Initiative (MURI) Center on Polymeric Smart Skin Materials through the Air Force Office of Scientific Research contract F49620-01-1-0364 (to G.E.K.). The diffractometer was funded by NSF grant 0087210, by Ohio Board of Regents grant CAP-491, and by YSU. S.J. and N.J.T. thank the National Science Foundation for financial support through grant NSF CHE-0717518.

Supporting Information Available: The X-ray crystallographic file in CIF format for the reported structure **5Pt**. ^{1}H, ^{13}C NMR, and IR spectra of **5Pt**, **8**, **9**, **10**, and **10Pt** and more details on the photophysical investigations. This material is available free of charge via the Internet at http://pubs.acs.org.

IC802041Z